Europace (2016) **18**, iv104–iv112
doi:10.1093/europace/euw356

SUPPLEMENT PAPER

Non-invasive, model-based measures of ventricular electrical dyssynchrony for predicting CRT outcomes

Christopher T. Villongco[1,2], David E. Krummen[2,3], Jeffrey H. Omens[1,2], and Andrew D. McCulloch[1,2]*

[1]Department of Bioengineering, University of California, 9500 Gilman Drive, La Jolla, San Diego, CA 92093-0412, USA; [2]Department of Medicine (Cardiology), University of California, 9500 Gilman Drive, La Jolla, San Diego, CA 92093-0613, USA; and [3]US Department of Veterans Affairs San Diego Healthcare System, 3350 La Jolla Village Drive, San Diego, CA 92161, USA

Received 1 April 2016; accepted after revision 2 August 2016

Aims Left ventricular activation delay due to left bundle branch block (LBBB) is an important determinant of the severity of dyssynchronous heart failure (DHF). We investigated whether patient-specific computational models constructed from non-invasive measurements can provide measures of baseline dyssynchrony and its reduction after CRT that may explain the degree of long-term reverse ventricular remodelling.

Methods and results LV end-systolic volume reduction (ΔESV_{LV}) measured by 2D trans-thoracic echocardiography in eight patients following 6 months of CRT was significantly ($P < 0.05$) greater in responders ($26 \pm 20\%$, $n = 4$) than non-responders ($11 \pm 16\%$, $n = 4$). LV reverse remodelling did not correlate with baseline QRS duration or its change after biventricular pacing, but did correlate with baseline LV endocardial activation measured by electroanatomic mapping ($R^2 = 0.71$, $P < 0.01$).

Patient-specific models of LBBB ventricular activation with parameters obtained by matching model-computed vectorcardiograms (VCG) to those derived from standard patient ECGs yielded LV endocardial activation times that correlated well with those measured from endocardial maps ($R^2 = 0.90$). Model-computed 3D LV activation times correlated strongly with the reduction in LVESV ($R^2 = 0.93$, $P < 0.001$). Computed decreases due to simulated CRT in the time delay between LV septal and lateral activation correlated strongly with ΔESV_{LV} ($R^2 = 0.92$, $P < 0.001$). Models also suggested that optimizing VV delays may improve resynchronization by this measure of activation delay.

Conclusions Patient-specific computational models constructed from non-invasive measurements can compute estimates of LV dyssynchrony and their changes after CRT that may be as good as or better than electroanatomic mapping for predicting long-term reverse remodelling.

Keywords Heart failure • Left bundle branch block • Cardiac resynchronization therapy • Computational modelling • Vectorcardiogram • Electroanatomic mapping

* Corresponding author. Tel: +1-858-534-2547. *E-mail address*: amculloch@ucsd.edu

What's new?

- Indices of ventricular electrical dyssynchrony estimated with 3D patient-specific electrophysiology models may predict LV reverse remodelling after CRT as well or better than similar metrics derived from invasive electroanatomic measurements.
- Model analyses suggest there is potential for patient-specific model-derived measures of ventricular dyssynchrony to assist in VV delay optimization.

Introduction

In patients with dyssynchronous heart failure (DHF), delayed ventricular electrical activation due to left bundle branch block (LBBB) gives rise to mechanical dyssynchrony, wasted work and reduced cardiac output.[1] QRS duration >120 ms remains the main criterion for electrical dyssynchrony used under current guidelines for selecting patients likely to benefit from cardiac resynchronization therapy (CRT) owing to its simplicity, non-invasiveness, and robustness in predicting survival rates.[2] Improved long-term survival after CRT is associated with improved systolic function and reverse left ventricular (LV) geometric remodelling.[3,4]

Although the goal of CRT is to improve mechanical pump function by restoring electrical synchrony, studies have shown that QRS shortening itself does not itself correlate with mechanical resynchronization,[5] and functional improvements in ejection fraction have been reported even with increased activation dispersion.[6] Moreover, an estimated 50% of HF patients with mechanical dyssynchrony present with normal QRS durations.[7] Hence, while severe electromechanical dyssynchrony is typically associated with prolonged QRS duration >150 ms, the degree of electromechanical dyssynchrony in patients with QRS durations <130 ms is less clear, and successful CRT may require more careful optimization of the pacing protocol.[8] Invasive electroanatomic mapping studies in humans[9–11] and dogs[12] have provided more complete pictures of LBBB activation patterns characterized by U-shaped activation wavefronts, variable LV endocardial breakthrough sites in the septum and prolonged transseptal and LV endocardial activation times. Such spatiotemporal information provides a more comprehensive, patient-specific assessment of dyssynchronous electrophysiologic substrate at baseline, which may be useful for guiding optimal CRT patient selection and delivery by identifying ideal lead locations in late-activated regions[13] and setting appropriate AV and VV delays.[14]

In recent work, patient-specific computational models of ventricular electrophysiology derived from measured ventricular anatomy and standard 12-lead ECGs[15] have been shown to reproduce endocardial activation times in patients with LBBB. These patient-specific models can also be used to simulate the effects of CRT pacing on activation patterns.[16] We investigated whether measures of electrical dyssynchrony derived from patient-specific electrophysiological models of LBBB and CRT pacing provide a viable non-invasive alternative to clinical measures of electrical dyssynchrony determined by electroanatomic mapping. We tested this hypothesis by comparing activation time delays derived from endocardial electrical mapping with those computed by patient-specific models in patients who received CRT. We found that specific measured metrics of LV activation delay that correlated with long-term reverse ventricular remodelling after CRT in these patients could also be reliably obtained with the models derived from standard ECG measurements. Moreover, the extent of reverse remodelling in patients was determined by the predicted degree of reduction in the model-derived dyssynchrony metric after simulated CRT. This reduction in dyssynchrony in the patent-specific models could be maximized by optimal choice of VV delay settings.

Methods

Clinical study

The patient cohort in this study has been described previously (Krishnamurthy *et al.* submitted for publication).[15] Eight male patients (aged 66 ± 11 years) with dilated cardiomyopathy, NHYA class III heart failure, prolonged QRS duration (135 ± 18 ms) left bundle branch ECG morphology and reduced left ventricular ejection fraction (LVEF) (28 ± 7%) were recruited from the Veteran's Administration San Diego Healthcare System (San Diego, CA). All patients gave informed consent to participate in the study approved by the Institutional Review Board. Dilated ventricular geometry was imaged by computed tomography (CT) ($n = 6$) or magnetic resonance (MR) ($n = 2$) when CT was unavailable. In patients with myocardial infarction ($n = 5$), scar region was localized by single-photon emission computed tomography (SPECT) (technetium sestamibi, ECAM-2, Siemens Medical Solutions, Hoffman Estates, IL) obtained at rest and stress states. LV volumes at baseline and 6-month follow up were computed by Simpson's method from 2D transthoracic echocardiographic (2D TTE) images of two- and four-chamber long-axis views (Sonos, Philips Medical IE33, Bothell, WA). LV reverse remodelling was quantified by the % change in end-systolic volume (ΔESV_{LV}) with respect to baseline. CRT response was defined by >10% decrease in LV end-systolic volume referred to baseline (positive and negative values indicate decrease and increase in volume, respectively).

Standard 12-lead body-surface ECGs were recorded during baseline LBBB and CRT over 5–6 beats at 1 kHz sampling rate. 3D vectorcardiograms (VCGs) were derived from the ECGs by the Kors transformation.[17] LV endocardial activation at baseline was obtained by the EnSite 3000 non-contact electroanatomic mapping system (Endocardial Solutions, St. Paul, MN, USA) using a bipolar roving catheter deployed by the typical trans-venous approach.[18] Local activation time was defined as the time interval between the onset of the QRS complex on simultaneously recorded body-surface ECGs and $-dV/dt_{max}$ of the largest negative deflection of voltage in the roving catheter electrogram. Local activation times from real (as opposed to interpolated or virtual) electrograms were considered for this study.

CRT-D devices were implanted with pace/sense leads placed on the right atria (lead A), RV apex (lead V) and the LV free wall (lead V) in the typical mid or posterior left lateral branch of the coronary sinus. Patient-specific lead positions were localized at corresponding anatomical locations of the geometric model by an expert electrophysiologist (D.E.K.) from bi-plane chest X-ray images. AV delays were programmed to 161.25 ± 21 ms (paced) and 121.25 ± 14 ms (sensed). The VV delay (defined as the time of the RV lead stimulus with respect to the initial LV lead stimulus) was programmed to 19.4 ± 16.6 ms by the QuickOpt algorithm (St. Jude Medical).[19]

Patient-specific electrophysiology model

Patient-specific models of ventricular electrophysiology were constructed using previously described methods.[15,16,20] In summary,

hexahedral cubic-Hermite finite element meshes[21,22] of ventricular geometry were fitted to segmented and triangulated CT and MR images using the Hexblender add-on (https://github.com/cmrglab/hexblender) for Blender 2.76 (Blender Foundation, Amsterdam, Netherlands, https://www.blender.org). Ventricular fibre architecture was approximated by diffeomorphic mapping of fibre, sheet and sheet-normal vectors from an atlas constructed from a diffusion-tensor MR (DT-MR) scan of *ex vivo* human ventricles using a log-Euclidean interpolation scheme[23] to the patient-specific geometry. Myocardial scar geometry was determined from the MIBI SPECT images and registered to each patient-specific mesh as a binary field of normal and scar tissue.

The myocardium was considered as a continuum with action potential propagation governed by monodomain reaction-diffusion and a transmembrane ionic current model of human ventricular myocytes.[24] Ion channel conductances for I_{to}, K_s and K_1 were decreased to approximate observed changes in AP morphology during HF.[16,25] The cardiac dipole or 'heart vector' ϕ_H resulting from the total source current density of a propagating action potential wave in the 3D myocardium was computed by:

$$\phi_H = -\int_{\Omega} \sigma_i \nabla \phi_t d\Omega$$

where σ_i is the intracellular conductivity, ϕ_t is the transmembrane potential, and Ω is the geometric domain of the ventricular myocardium.

Simulations of LBBB and CRT activation

The LBBB activation pattern was estimated by the depolarization simulation that minimized the angular deviation between the VCG QRS complex computed by the model and the Kors VCG QRS complex derived from measured ECG by adjusting an ectopic stimulus site constrained to lie within the RV free wall, apex, and septum subendocardium to allow for observed LV breakthrough sites.[10,11] Myocardial conductivity in the endocardial and bulk layers was simultaneously adjusted to match the total duration of the measured VCG QRS duration to within 10 ms of the measured QRS duration during biventricular pacing; an additional 10 ms was allowed to account for capture delay which was not functionally reproduced in the model. Conductivity in myocardial infarct regions was adjusted as a percentage of the bulk myocardial conductivity. Endocardial activation times were previously validated against electroanatomic measurements in three patients with LBBB.[15]

Using the same conductivity parameters as at baseline, CRT activation was simulated by applying stimuli at the prescribed lead locations in the RV apex and LV lateral wall. To account for functional lead capture delay mechanisms that are not included in the model, the effective VV delay was allowed to vary within ±20 ms (10 ms uncertainty per lead) of the measured VV delay. The CRT depolarization simulation that resulted in a total activation time within 10 ms of the measured CRT QRS duration was approximated as the activation pattern. Finally, we evaluated the variation of LV electrical resynchronization as a function of VV delay swept over the range of −80 ms to +80 ms in steps of 5 ms.

Definitions of dyssynchrony measures

We define several metrics of global and regional electrical dyssynchrony derived from measured and simulated ECGs/VCGs and local LV activation times. Dyssynchrony metrics derived from clinical data were defined as (1) the maximum QRS duration (ms) recorded by body surface ECG leads; and (2) LV endocardial activation time AT_{LVendo} defined as the difference between the latest and earliest times normalized by the latest activated site to account for inter-patient variability in ventricular size and myocardial conductivity (*Figure 1*).

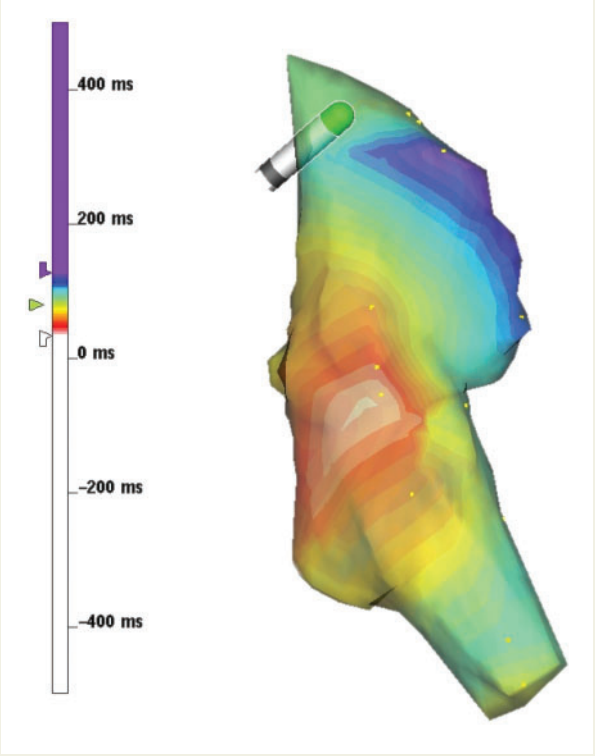

Figure 1 Electroanatomic map of baseline LBBB activation in the LV endocardium in a representative patient (BiV7). The LV breakthrough site occurs in the LV mid septum (27 ms, red) and activation terminates baso-laterally (133 ms, blue). LV endocardial activation time AT_{LVendo} was computed as the delay between the earliest and latest activated sites as a fraction of the latest activated site (~80% shown).

In the models, activation times were evaluated on the 3D LV geometry from endocardium to epicardium. Indices of dyssynchrony derived from the models were defined as (1) total biventricular activation time, AT_{tot} (analogous to QRS duration (ms)); (2) LV endocardial activation time, AT_{LVendo}; and (3) 3D LV activation time, AT_{LV}, where the earliest and latest sites of activation could occur at the interventricular septum and the LV epicardium. We computed the time courses of activated myocardial mass in the septum and LV lateral wall, each normalized to the total mass of its respective region (*Figure 3*). At each time point, we defined the instantaneous activation mass dyssynchrony as the difference between the two regions. Summing the area under the curve and normalizing by the total duration, we computed the mean LV lateral/septal activation dyssynchrony, mAT_{STLV}. See *Table 1* for a summary of all dyssynchrony metric definitions.

Statistics

Two-tailed unpaired *T*-tests were used to compare measured and simulated differences between responders and non-responders. The significance of the relationship between LV reverse remodelling and dyssynchrony metrics was computed by linear regression using Pearson's correlation coefficient with associated significance values for $n = 8$. In both tests, P value < 0.05 was considered statistically significant. Average data are reported as mean ± SD.

Table 1 Summary of dyssynchrony metric definitions and strengths of correlation to LV reverse remodelling

Electrical dyssynchrony Index	Definition	Clinical measurement		Patient-specific model	
		R^2	*P* value	R^2	*P* value
QRS duration	Longest ECG QRS complex	0.0	–	0.0	–
LV endocardial activation time (AT_{LVendo})	$\frac{LVendo_{late}-LVendo_{early}}{LVendo_{late}}$	0.71	<0.01	0.78	<0.001
LV activation time (AT_{LV})	$\frac{LV_{late}-LV_{early}}{LV_{late}}$	NA	NA	0.93	<0.001
mean LV lateral/septal delay time (ΔmAT_{STLV})	$\frac{LVlat_{mean}-ST_{mean}}{AT_{tot}}$	NA	NA	0.92	<0.001

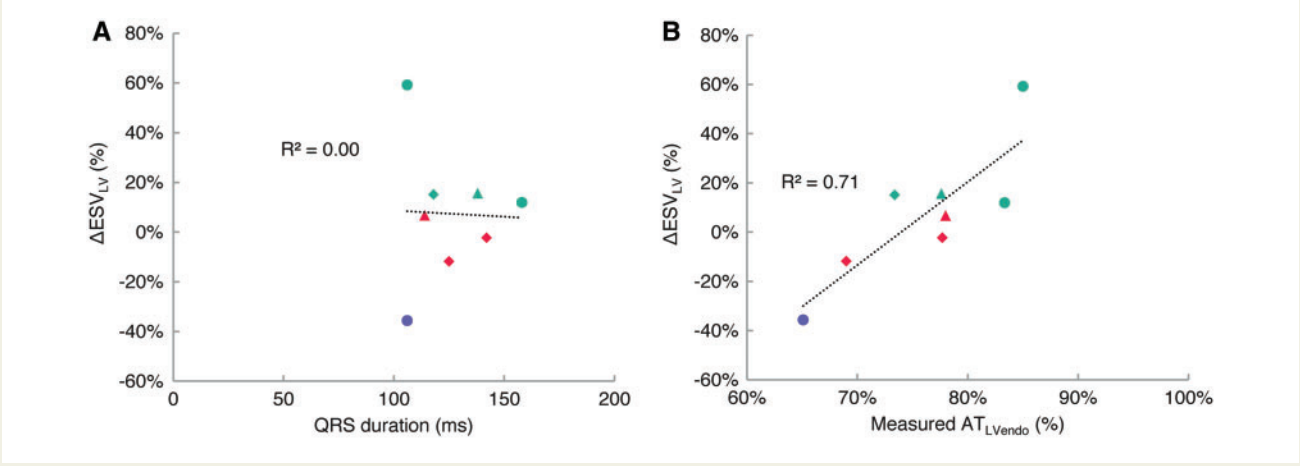

Figure 2 Correlation between LV reverse remodelling and estimates of dyssynchrony derived from measurements: QRS duration derived from ECG (*A*) and LV endocardial activation AT_{LVendo} derived from electroanatomic maps (*B*). LV reverse remodelling has no correlation to baseline QRS duration, but is significantly correlated to AT_{LVendo} ($P < 0.01$). Turquoise—responder; red—non-responder; lilac—clinical non-responder; triangle—myocardial infarction; diamond—myocardial infarct + mitral regurgitation.

Results

LV reverse remodelling outcomes of CRT

Among the eight patients, the reduction in LV end-systolic volume (ΔESV_{LV}) at 6-month follow up averaged 7 ± 25% (26 ± 20% in responders; −11 ± 16% in non-responders; $P = 0.05$). There were four echocardiographic responders ($\Delta ESV_{LV} > 10\%$) and four non-responders. The responders were patients BiV6 (+50 mL; +59%), BiV3 (+14 mL; +16%), BiV5 (+32 mL; +15%) and BiV1 (+17 mL; +12%). The non-responders were patients BiV8 (+8 mL; +7%), BiV2 (−3 mL; −2%), BiV4 (−22 mL; −12%) and BiV7 (−55 mL; −36%). BiV7 was also a clinical non-responder.

Clinical measures of baseline dyssynchrony correlate with outcomes

Measured baseline QRS duration was 136 ± 17 ms (140 ± 20 ms in responders; 132 ± 14 ms in non-responders; $P = 0.57$). LV reverse remodelling and baseline QRS durations showed no correlation (*Figure 2A*). The change in QRS duration following acute biventricular pacing (positive values indicate QRS reduction) was −4 ± 32 ms (1 ± 39 ms in responders; −8 ± 24 ms in non-responders; $P = 0.76$). Reverse remodelling and the change in QRS duration also showed no correlation.

The total time for LV endocardial activation AT_{LVendo} was computed from the earliest and latest measured activation times of the electroanatomic maps. The earliest activated time was 27 ± 7 ms, (25 ± 7 ms for responders; 31 ± 5 ms for non-responders; $P = 0.28$) and occurred at anterior, mid and posterior sites in the septum. The latest activation time was 117 ± 17 ms (120 ± 12 ms for responders; 114 ± 20 ms for non-responders; $P = 0.67$) and occurred at basal lateral and postero-lateral sites. The total AT_{LVendo} was 76 ± 6% (80 ± 5% for responders; 72 ± 6% for non-responders; $P = 0.12$). We found a significant correlation between remodelling and clinical measurement-derived AT_{LVendo} ($R^2 = 0.71$, $P < 0.01$) (*Figure 2B*).

Model-derived measures of baseline dyssynchrony correlate with outcomes

Total AT_{LVendo} was 75 ± 7% (79 ± 3% in responders; 70 ± 7% in non-responders; $P = 0.07$). We found good agreement in the LV endocardial activation times between electroanatomic map measurements and model estimates ($R^2 = 0.90$) (*Figure 4A*). Comparison between ΔESV_{LV} and model-predicted LV endocardial times (*Figure 4B*) showed agreement ($R^2 = 0.78$, $P < 0.001$) with the measurements in *Figure 2B*.

We derived the same dyssynchrony metrics from the patient-specific model-computed 3D activation patterns during LBBB.

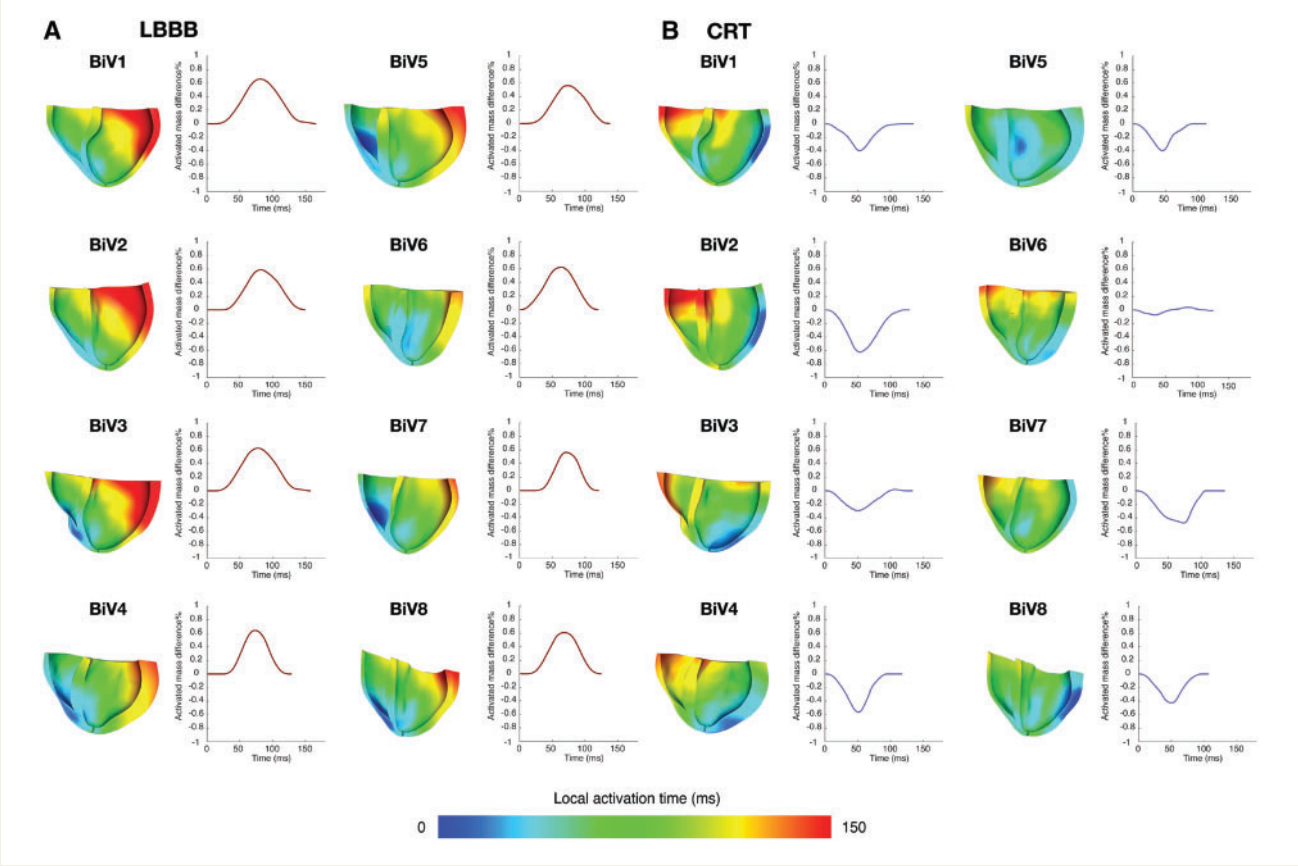

Figure 3 Sectioned view of LBBB and CRT activation patterns estimated from electrophysiology models. LBBB activation patterns feature depolarization beginning in the RV free wall, crossing the septum and terminating in the basolateral wall. During biventricular pacing, depolarization begins in the LV free wall and septum and progresses basally and to the right ventricle. Inter-patient variations in ventricular geometry, myocardial conductivity, lead placement and VV delay give rise to different degrees of resynchronization quantified by the time course of the difference in activated mass fraction between the septum and LV lateral wall. The mean magnitude mAT_{STLV} is computed by normalizing the area under the curves by the total duration during LBBB (red) and CRT (blue). The best responder, BiV6, has largest peak mAT_{STLV} at baseline and achieved optimal elimination of mAT_{STLV}. All other patients experienced reversal of dyssynchrony due to pacing.

Activation patterns for all patients are shown in *Figure 3*. We first compared LV endocardial activation times between the model and electroanatomic measurements. The earliest activation time in the LV endocardium was 33 ± 7 ms (29 ± 6 ms in responders; 36 ± 6 ms in non-responders; $P = 0.21$). The latest activation time was 132 ± 19ms (141 ± 19 ms in responders; 124 ± 15 ms in non-responders; $P = 0.25$). The total AT_{LVendo} was 75 ± 7% (79 ± 3% in responders; 70 ± 7% in non-responders; $P = 0.07$). We found good agreement in the LV endocardial activation times between electroanatomic map measurements and model results ($R^2 = 0.90$, $P < 0.001$) (*Figure 4A*). Comparing ΔESV_{LV} and model-computed LV endocardial times (*Figure 4B*) showed a significant correlation ($R^2 = 0.78$, $P < 0.001$) that was highly consistent with the relationship between the measurements shown in *Figure 2B*.

Next we determined the correlation between dyssynchrony in the 3D LV and functional outcomes. We considered the LV "surfaces" at which action potential waves may first break to include the posterior, lateral, and anterior epicardial surfaces and the interventricular septum surface in the RV. The earliest LV activation time was 17 ± 8 ms (11 ± 5 ms in responders; 22 ± 5 ms in non-responders; $P = 0.04$). The latest LV activation time was 138 ± 17 ms (151 ± 14 ms in responders; 126 ± 7 ms in non-responders; $P = 0.03$). Total LV activation duration AT_{LV} was 86 ± 7% (91 ± 4% in responders; 81 ± 4% in non-responders; $P = 0.03$). We found a very strong and significant relationship between AT_{LV} and ΔESV_{LV} reduction ($R^2 = 0.93$, $P < 0.001$) (*Figure 5A*).

Model measures of resynchronization correlate with outcomes

Acute biventricular pacing activation patterns were evaluated from the patient-specific CRT models to derive mAT_{STLV} and examine its correlation to LV reverse remodelling. The change in QRS duration (LBBB−CRT; reduction is positive) was 3 ± 15 ms (7 ± 10 ms in responders; −1 ± 17 ms in non-responders; $P = 0.52$). At baseline, the mean activation time of the septum was 60 ± 7 ms (59 ± 8 ms in responders; 61 ± 6 ms in non-responders; $P = 0.64$). The mean activation time of the LV lateral wall was 94 ± 9 ms (96 ± 9 ms in

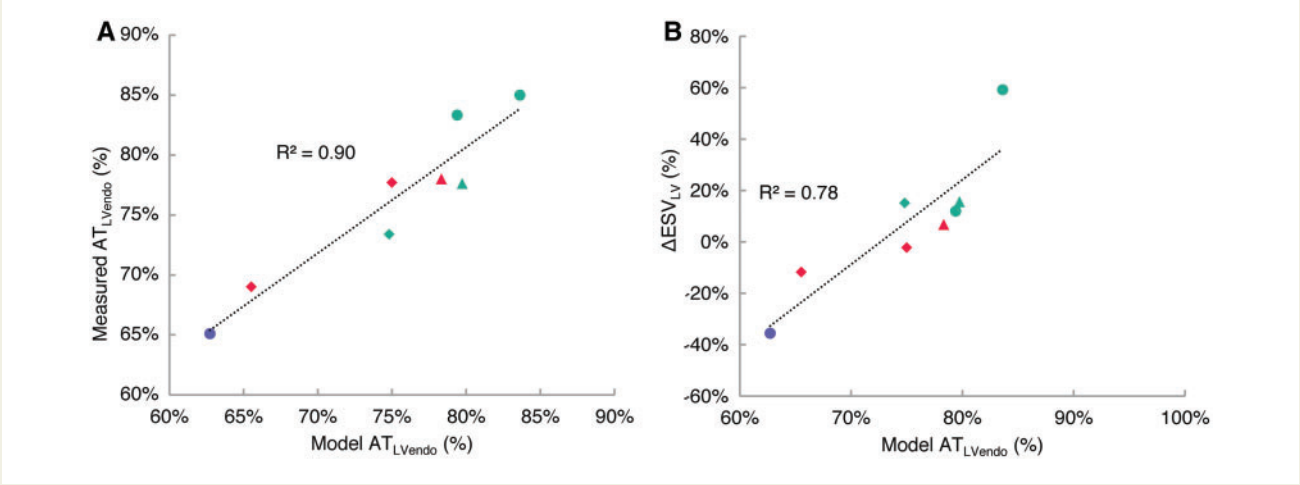

Figure 4 Comparison between LV endocardial activation times between measurements and models show good agreement ($R^2 = 0.90$) (*A*). LV endocardial activation time ATLVendo relates to LV reverse remodelling comparably with the same metric derived from electroanatomic measurements in *Figure 2(B)* ($R^2 = 0.78$; $P < 0.001$) (*B*). Turquoise—responder; red—non-responder; lilac—clinical non-responder; triangle—myocardial infarction; diamond—myocardial infarct + mitral regurgitation.

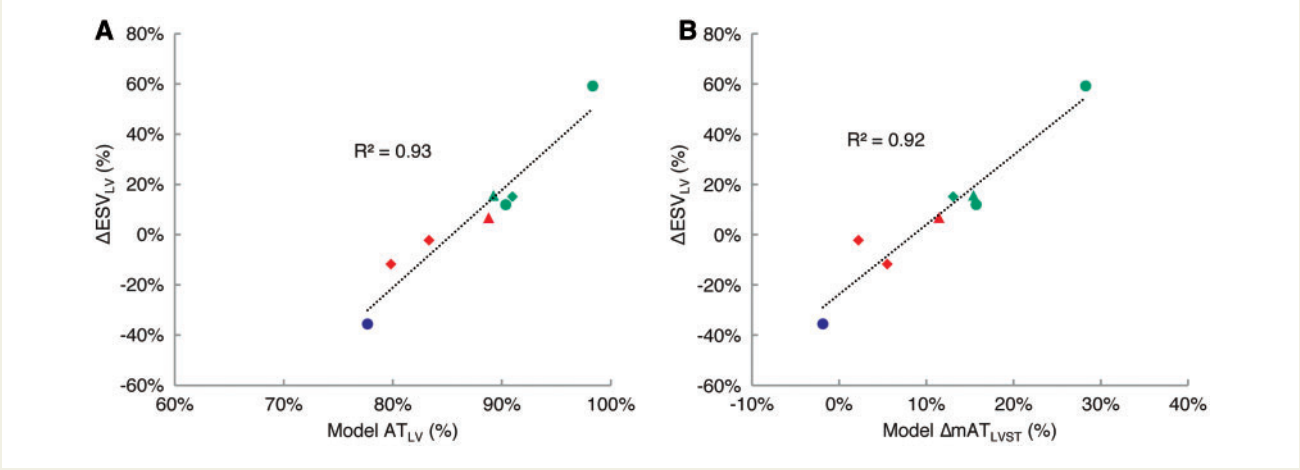

Figure 5 At baseline LBBB, LV reverse remodelling is strongly correlated to LV activation delay AT_{LV} ($R^2 = 0.93$; $P < 0.001$) (*A*). LV reverse remodelling is also strongly correlated to the resynchronization estimated by ΔmAT_{STLV} following acute CRT ($R^2 = 0.93$; $P < 0.001$) (*B*). Turquoise—responder; red—non-responder; lilac—clinical non-responder; triangle—myocardial infarction; diamond—myocardial infarct + mitral regurgitation.

responders; 92 ± 8 ms in non-responders; $P = 0.56$). Baseline mAT_{STLV} (positive values indicate right-to-left delay) was then 24 ± 3% (26 ± 2% in responders; 23 ± 2% in non-responders; $P = 0.14$). During biventricular pacing, the mean activation time of the septum was 63 ± 7 ms (60 ± 5 ms in responders; 66 ± 8 ms in non-responders; $P = 0.31$). The mean activation time of the LV lateral wall was 45 ± 6 ms (48 ± 5 ms in responders; 41 ± 5 ms in non-responders; $P = 0.12$). Pacing caused significant ΔmAT_{STLV} (reduction is positive) by 11 ± 8%, (18 ± 6% in responders; 4 ± 5% in non-responders; $P = 0.02$) and showed a strong correlation with ΔESV_{LV} ($R^2 = 0.92$, $P < 0.001$) (*Figure 5B*).

Degree of resynchronization varies as a function of VV delay

We estimated the sensitivity of resynchronization to VV delays by computing LV lateral/septal mean regional delay from simulations varying VV delay between −80 ms and 80 ms in steps of 5 ms; delay times are defined as $Vt_{LV} - Vt_{RV}$. *Figure 6* shows the variation of mAT_{STLV} as a function of VV delay for each patient. Baseline values of mAT_{STLV} were 24 ± 3% (26 ± 2% in responders; 23 ± 2% in non-responders; $P = 0.14$). The curves feature inter-patient variability of VV delay regimes where the change varies linearly (near nominal VV delay = 0 ms settings) and plateaus (at extreme VV delays). The

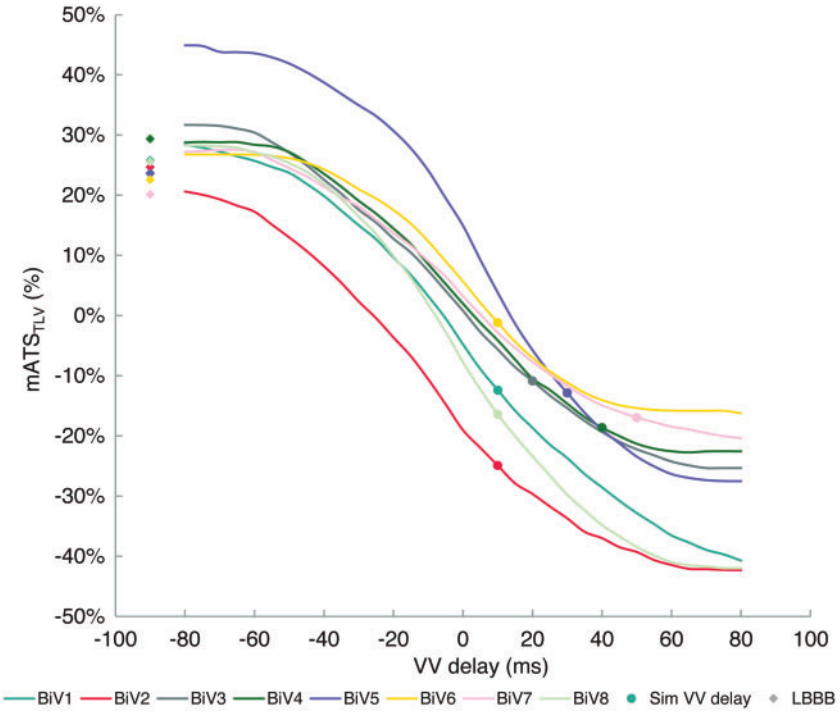

Figure 6 Patient-specific variation of mAT$_{STLV}$ as a function of VV delay (coloured curves). Baseline LBBB values are shown by diamond markers in corresponding colours. The zero crossing of each curve predicts the VV delay at which optimal resynchronization is achieved due to inter-patient variation of ventricular geometry, myocardial conduction, lead placement, and scar burden. The zero crossing varies in the vicinity of VV delay 0 ± 12 ms (5 ± 8 ms in responders; -6 ± 12 ms in non-responders; $P = 0.23$). The curve for BiV2 suggests RV pre-excitation due to the presence of postero-septal scar near the RV lead. Biventricular pacing with VV delay > 0 (LV pre-excitation) introduces left-to-right dyssynchrony, reversing mAT$_{STLV}$ ($-15 \pm 7\%$ overall; $-9 \pm 2\%$ in responders; $-20 \pm 3\%$ in non-responders; $P = 0.02$). Optimal resynchronization was achieved for the best responder, BiV6. Non-responders had significant overshoot compared to responders.

maximum slope in the linear region was virtually the same among all patients 8 ± 2%/ms in the vicinity of VV delay -2 ± 4 ms, indicating similar functional 'viability' for resynchronization among all patients.

Estimated values of dyssynchrony using the effective VV delay are shown by markers on the curves. Biventricular pacing reversed dyssynchrony in the left-to-right direction to $-15 \pm 7\%$ ($-9 \pm 2\%$ in responders; $-20 \pm 3\%$ in non-responders; $P = 0.02$). Non-responders exhibited a significantly greater amount of dyssynchrony reversal introduced by pacing. Optimal resynchronization at the zero crossing of the curves at which dyssynchrony is eliminated also varied among the patients in the vicinity of VV delay 0 ± 12 ms (5 ± 8 ms in responders; -6 ± 12 ms in non-responders; $P = 0.23$). These characteristics are determined by the conductivity, LV geometry and size, and relative locations of RV and LV V leads. BiV6 was the best responder and was closest to optimal resynchronization. BiV2 had the most negative zero crossing and suggests that RV pre-excitation could improve outcome. In the case of BiV2, the RV lead was placed in the vicinity of a postero-septal scar, and the pre-excitation accounts for slowed conduction through the scar region.

Discussion

In this study, we found that estimates of ventricular dyssynchrony computed from patient-specific models optimized to match VCGs derived from standard ECG measurements and validated against early and late endocardial activation times from electroanatomic maps correlated strongly with long-term reverse remodelling responses to CRT. On one hand, measured baseline QRS duration and its change after acute biventricular pacing had no correlation to remodelling in this set of patients. On the other hand, baseline AT$_{LVendo}$ derived from electroanatomic mapping differed more significantly between responders and non-responders and was correlated strongly with reverse remodelling. We are unaware of any studies to date that have conducted a thorough investigation of the relationship between remodelling and LV delay at the endocardium as most studies focus on outcomes related to acute hemodynamic improvement. Using patient-specific models of LBBB activation, we computed values of AT$_{LVendo}$ that agreed with our clinical measurements and showed a comparable correlation with LV reverse remodelling. The average model-derived AT$_{LVendo}$ was $75 \pm 7\%$ which is in agreement with previous electroanatomic mapping studies

of LBBB activation.[11] We also found good agreement between measured and simulated early and late activated sites in anterior, mid and posterior positions of the LV septum and free wall, respectively.

We then used the models to obtain the total activation time of the entire LV, rather than just the endocardium, and found a significantly stronger correlation with reverse remodelling, suggesting the importance of considering 3D activated myocardial mass as it relates to electrical and mechanical dyssynchrony.[26] Our 3D analysis further showed that the activation time across the septum between the earliest activated sites in the RV and LV was significantly different between responders and non-responders (16 ± 3 ms overall; 18 ± 2 ms in responders; 14 ± 1 ms in non-responders; $P = 0.01$). Furthermore, the earliest septal activation time in the RV side was also significantly different between responders and non-responders, (17 ± 8 ms overall; 11 ± 5 ms in responders; 22 ± 5 ms in non-responders; $P = 0.04$), whereas the latest LV activation time on the epicardium was not (138 ± 16 ms overall; 146 ± 18 ms in responders; 131 ± 11 ms in non-responders; $P = 0.29$). These results indicate that baseline septal activation may be an important disease substrate to consider due to its involvement in intra- and interventricular dyssynchrony. In our models, earlier activation of the septum as a fraction of total LV activation time increases LV intraventricular delay. Trans-septal activation time, defined as the delay between the onset of the QRS complex and earliest activation at the LV endocardial electrogram, has been identified as an important feature of LBBB in electroanatomic mappings studies in humans.[10,11] Trans-septal times were reported to lie between two populations: <20 ms and >40 ms in the remainder. Our models are consistent with timings in the shorter population after accounting for $\sim$10 ms delay between initial depolarization in the RV and the onset of the QRS complex. To the best of our knowledge, the significance of baseline trans-septal activation time in relation to LV reverse remodelling has not been examined.

In biventricular pacing simulations, global electrical delay reduction defined by ΔAT_{tot} ($3 \pm 7\%$) did not correlate with reduction in regional delay defined by ΔmAT_{STLV} ($11 \pm 9\%$), suggesting that regional resynchronization is not reflected by global resynchronization. Similar findings have been shown in a canine study by Lumens *et al.*[27] where biventricular pacing reduced the mean QRS duration by 5% and mean LV activation time (defined as the delay between LV epicardial activation and RV septal activation) by 12% compared with baseline. Interestingly, we found a slight increase in mean ΔAT_{LVendo} ($-6 \pm 9\%$) with biventricular pacing. This finding is similar to that of Strik *et al.*[12] which showed that AT_{LVendo} remained unchanged during LBBB and biventricular pacing in dogs. LV pre-excitation and larger size of dilated human hearts compared with dogs may explain the increased AT_{LVendo}.

Finally, the models were able to characterize the extent of electrical resynchronization as a function of VV delay. The analysis suggested that VV delays producing maximal acute hemodynamic function were longer than required to optimally minimize electrical dyssynchrony, and instead resulted in overshot left-to-right dyssynchrony ($-15 \pm 7\%$ overall; $-9 \pm 2\%$ in responders; $-20 \pm 3\%$ in non-responders; $P = 0.02$) in all but the best CRT responder. Biventricular pacing has been shown to introduce dyssynchrony in a human study,[28] and can potentially cause harm in patients with QRS < 130 ms as in the EchoCRT trial.[8] This fact highlights the importance of optimal delivery of biventricular pacing, particularly for mildly symptomatic HF patients (QRS duration > 120 ms) who are typically less likely responders but may still benefit by LV reverse remodelling and long-term survival.[29] The notion that optimal CRT should maximize acute functional hemodynamic improvement has been challenged by studies that have shown that baseline LV dP/dt_{max}, but not its change, predicts long-term clinical outcomes to CRT.[30,31]

Limitations

The sample size of this patient cohort is small, and the relationships between measured electrical dyssynchrony and reverse remodelling demonstrated here should be interpreted as preliminary. We have, however, demonstrated that model-predicted electrical dyssynchrony metrics at baseline and their acute change due to biventricular pacing are consistent with our own measurements and previous studies; the associated degree of mechanical dyssynchrony was not considered in this modelling work but warrants further investigation. The fact that our small cohort included an extreme responder and non-responder contributed to the strength of the correlations. Larger, randomized and blinded studies are needed to substantiate our findings and define threshold values for predictive metrics. Moreover, it is important to acknowledge that our simulated effects of altered VV delay are only model predictions; they have not been tested in the clinic. Finally, we did not examine correlations between model dyssynchrony and ECG morphology due to incomplete patient information on torso lead positions. A recent in silico study by Nguyen *et al.*[32] showed that ECG features such as notching and T-wave area are sensitive to lead placement. Further modelling studies should seek to find novel ECG features for improved clinical estimates of baseline dyssynchrony.

Conclusion

Indices of ventricular electrical dyssynchrony estimated with 3D patient-specific computational models derived from standard ECG measurements may predict LV reverse remodelling after CRT as well or better than similar metrics computed from invasive electroanatomic measurements. Model analyses suggest that there is potential for patient-specific model-derived measures of ventricular dyssynchrony to assist in VV delay optimization.

Acknowledgements

We thank Jeff van Dorn for providing technical support in running the Continuity software.

Funding

This work was supported by National Institutes of Health Grants 1R01HL96544 (to A.D.M.), 1R01HL105242 (to A.D.M.), 1R01HL121754 (to A.D.M.), 8P41GM103426 (to R. Amaro and A.D.M.) and P50GM094503 (to D. Beard and A.D.M.).

Conflicts of interest: Patent applications related to the technology described here have been submitted in the United States ('Compositions and methods for patient-specific modelling to predict outcomes of cardiac resynchronization therapy,' serial no. P00015-268P01; 'Patient-specific modelling of ventricular activation pattern using surface ECG-derived vectorcardiogram in bundle branch block,' serial no. PCT/US15/36788). A.D.M and J.H.O are co-founders, scientific advisors and equity-holders in

Insilicomed, Inc., a licensee of UC San Diego software used in this research. Insilicomed, Inc. had no involvement at all in design, performance, analysis or funding of the present study. This relationship has been disclosed to, reviewed, and approved by the University of California San Diego in accordance with its conflict of interest policies.

References

1. Prinzen FW, Augustijn CH, Arts TH, Allessie MA, Reneman RS. Redistribution of myocardial fiber strain and blood flow by asynchronous activation. *Am J Physiol-Heart Circ Physiol* 1990 **1**;259:H300–8.
2. Gasparini M, Leclercq C, Yu CM, Auricchio A, Steinberg JS, Lamp B *et al.* Absolute survival after cardiac resynchronization therapy according to baseline QRS duration: a multinational 10-year experience: data from the Multicenter International CRT Study. *Am Heart J* 2014 **28**;167:203–9.
3. Solomon SD, Foster E, Bourgoun M, Shah A, Viloria E, Brown MW *et al.* MADIT-CRT Investigators. Effect of cardiac resynchronization therapy on reverse remodeling and correlation to outcome multicenter automatic defibrillator implantation trial: cardiac resynchronization therapy. *Circulation* 2010;**122**:985–92.
4. Yu CM, Bleeker GB, Fung JW, Schalij MJ, Zhang Q, van der Wall EE *et al.* Left ventricular reverse remodeling but not clinical improvement predicts long-term survival after cardiac resynchronization therapy. *Circulation* 2005;**112**:1580–6.
5. Kass DA, Chen CH, Curry C, Talbot M, Berger R, Fetics B *et al.* Improved left ventricular mechanics from acute VDD pacing in patients with dilated cardiomyopathy and ventricular conduction delay. *Circulation* 1999;**99**:1567–73.
6. Leclercq C, Faris O, Tunin R, Johnson J, Kato R, Evans F *et al.* Systolic improvement and mechanical resynchronization does not require electrical synchrony in the dilated failing heart with left bundle-branch block. *Circulation* 2002;**106**:1760–3.
7. Yu CM, Lin H, Zhang Q, Sanderson JE. High prevalence of left ventricular systolic and diastolic asynchrony in patients with congestive heart failure and normal QRS duration. *Heart* 2003;**89**:54–60.
8. Ruschitzka F, Abraham WT, Singh JP, Bax JJ, Borer JS, Brugada J *et al.* Cardiac-resynchronization therapy in heart failure with a narrow QRS complex. *N Engl J Med* 2013;**369**:1395–405.
9. Fantoni C, Kawabata M, Massaro R, Regoli F, Raffa S, Arora V *et al.* Right and left ventricular activation sequence in patients with heart failure and right bundle branch block: a detailed analysis using three-dimensional non-fluoroscopic electroanatomic mapping system. *J Cardiovasc Electrophysiol* 2005;**16**:112–9.
10. Auricchio A, Fantoni C, Regoli F, Carbucicchio C, Goette A, Geller C *et al.* Characterization of left ventricular activation in patients with heart failure and left bundle-branch block. *Circulation* 2004;**109**:1133–9.
11. Rodriguez L, Timmermans C, Nabar A, Beatty G, Wellens HJ. Variable patterns of septal activation in patients with left bundle branch block and heart failure. *J Cardiovasc Electrophysiol* 2003;**14**:135–41.
12. Strik M, van Deursen CJ, van Middendorp LB, van Hunnik A, Kuiper M, Auricchio A *et al.* Transseptal conduction as an important determinant for cardiac resynchronization therapy, as revealed by extensive electrical mapping in the dyssynchronous canine heart. *Circulation: Arrhythm Electrophysiol* 2013;**6**:682–9.
13. Rad MM, Blaauw Y, Dinh T, Pison L, Crijns HJ, Prinzen FW *et al.* Left ventricular lead placement in the latest activated region guided by coronary venous electroanatomic mapping. *Europace* 2015;**17**:84–93.
14. Bogaard MD, Meine M, Tuinenburg AE, Maskara B, Loh P, Doevendans PA. Cardiac resynchronization therapy beyond nominal settings: who needs individual programming of the atrioventricular and interventricular delay? *Europace* 2012;**14**:1746–53.
15. Villongco CT, Krummen DE, Stark P, Omens JH, McCulloch AD. Patient-specific modeling of ventricular activation pattern using surface ECG-derived vectorcardiogram in bundle branch block. *Prog Biophys Mol Biol* 2014;**115**:305–13.
16. Aguado-Sierra J, Krishnamurthy A, Villongco C, Chuang J, Howard E, Gonzales MJ *et al.* Patient-specific modeling of dyssynchronous heart failure: a case study. *Prog Biophys Mol Biol* 2011;**107**:147–55.
17. Kors JA, Van Herpen G, Sittig AC, Van Bemmel JH. Reconstruction of the Frank vectorcardiogram from standard electrocardiographic leads: diagnostic comparison of different methods. *Eur Heart J* 1990;**11**:1083–92.
18. Schilling RJ, Peters NS, Davies DW. Simultaneous endocardial mapping in the human left ventricle using a noncontact catheter comparison of contact and reconstructed electrograms during sinus rhythm. *Circulation* 1998;**98**:887–98.
19. Kamdar R, Frain E, Warburton F, Richmond L, Mullan V, Berriman T *et al.* A prospective comparison of echocardiography and device algorithms for atrioventricular and interventricular interval optimization in cardiac resynchronization therapy. *Europace* 2010;**12**:84–91.
20. Krishnamurthy A, Villongco CT, Chuang J, Frank LR, Nigam V, Belezzuoli E *et al.* Patient-specific models of cardiac biomechanics. *J Comput Phys* 2013;**244**:4–21.
21. Nielsen PM, Le Grice IJ, Smaill BH, Hunter PJ. Mathematical model of geometry and fibrous structure of the heart. *Am J Physiol-Heart Circ Physiol* 1991;**260**:H1365–78.
22. Gonzales MJ, Sturgeon G, Krishnamurthy A, Hake J, Jonas R, Stark P *et al.* A three-dimensional finite element model of human atrial anatomy: new methods for cubic Hermite meshes with extraordinary vertices. *Med Image Anal* 2013;**17**:525–37.
23. Arsigny V, Fillard P, Pennec X, Ayache N. Log-Euclidean metrics for fast and simple calculus on diffusion tensors. *Magn Reson Med* 2006;**56**.2:411–21.
24. ten Tusscher KHWJ, Panfilov AV. Alternans and spiral breakup in a human ventricular tissue model. *Am J Physiol-Heart Circ Physiol* 2006;**291**.3:H1088–100.
25. Priebe L, Beuckelmann DJ. Simulation study of cellular electric properties in heart failure. *Circ Res* 1998;**82**:1206–23.
26. Auricchio A, Yu CM. Beyond the measurement of QRS complex toward mechanical dyssynchrony: cardiac resynchronisation therapy in heart failure patients with a normal QRS duration. *Heart* 2004;**90**:479.
27. Lumens J, Ploux S, Strik M, Gorcsan J, Cochet H, Derval N *et al.* Comparative electromechanical and hemodynamic effects of left ventricular and biventricular pacing in dyssynchronous heart failure: electrical resynchronization versus left–right ventricular interaction. *J Am Coll Cardiol* 2013;**62**:2395–403.
28. Ploux S, Eschalier R, Whinnett ZI, Lumens J, Derval N, Sacher F *et al.* Electrical dyssynchrony induced by biventricular pacing: implications for patient selection and therapy improvement. *Heart Rhythm* 2015;**12**:782–91.
29. Gold MR, Daubert C, Abraham WT, Ghio S, Sutton MS, Hudnall JH *et al.* The effect of reverse remodeling on long-term survival in mildly symptomatic patients with heart failure receiving cardiac resynchronization therapy: results of the REVERSE study. *Heart Rhythm* 2015;**12**:524–30.
30. Bogaard MD, Houthuizen P, Bracke FA, Doevendans PA, Prinzen FW, Meine M *et al.* Baseline left ventricular dP/dt_{max} rather than the acute improvement in dP/dt_{max} predicts clinical outcome in patients with cardiac resynchronization therapy. *EurJ Heart Fail* 2011;**13**:1126–32.
31. Suzuki H, Shimano M, Yoshida Y, Inden Y, Muramatsu T, Tsuji Y *et al.* Maximum derivative of left ventricular pressure predicts cardiac mortality after cardiac resynchronization therapy. *Clin Cardiol* 2010;**33**:E18–23.
32. Nguyên UC, Potse M, Regoli F, Caputo ML, Conte G, Murzilli R *et al.* An in-silico analysis of the effect of heart position and orientation on the ECG morphology and vectorcardiogram parameters in patients with heart failure and intraventricular conduction defects. *J Electrocardiol* 2015;**48**:617–25.